SCANNING VOL. 37, 179–185 (2015)

Leucine-Rich Amelogenin Peptide (LRAP) as a Surface Primer for Biomimetic Remineralization of Superficial Enamel Defects: An *In-Vitro* Study

Farhad Shafiei,[1] Bagheri G. Hossein,[1] Mohammad M. Farajollahi,[2] Moztarzadeh Fathollah,[3] Behroozibakhsh Marjan,[1] and Jafarzadeh Kashi Tahereh[4]

[1]Department of Dental Biomaterials, School of Dentistry/Research Center for Science and Technology in Medicine, Tehran University of Medical Sciences, Northern Kargar str., Hakim Highway, Tehran, Iran
[2]Department of Medical Biotechnology, Faculty of Allied Medicine/Cellular and Molecular Research Center, Iran University of Medical Sciences, Hemmat Highway, Tehran, Iran
[3]Faculty of Biomedical Engineering (Center of Excellence), Amirkabir University of Technology, Biomaterials Group, Amirkabir University of Technology, Hafez str., Tehran, Iran
[4]Department of Dental Biomaterials, School of Dentistry, Iranian Tissue Bank & Research Center, Research Center for Science and Technology, Tehran University of Medical Sciences, Northern Kargar str., Hakim Highway, Tehran, Iran

Summary: This study was carried out to obtain more information about the assembly of hydroxyapatite bundles formed in the presence of Leucine-Rich Amelogenin Peptide (LRAP) and to evaluate its effect on the remineralization of enamel defects through a biomimetic approach. One or 2 mg/mL LRAP solutions containing 2.5 mM of Ca^{+2} and 1.5 mM phosphate were prepared (pH = 7.2) and stored at 37 °C for 24 h. The products of the reaction were studied using atomic force microscopy (AFM), transmission electron microscopy (TEM), and selected area electron diffraction (SAED). Vickers surface microhardness recovery (SMR%) of acid-etched bovine enamel, with or without LRAP surface treatment, were calculated to evaluate the influence of peptide on the lesion remineralization. Distilled water and 1 or 2 mg/mL LRAP solution (pH = 7.2) were applied on the lesions and the specimens were incubated in mineralization solution (2.5mM Ca^{+2}, 1.5mM PO_4^{-3}, pH = 7.2) for 24 h. One-way ANOVA and Tukey's multi-comparison tests were used for statistical analysis. The pattern of enamel surface repair was studied using FE-SEM. AFM showed the formation of highly organized hierarchical structures, composed of hydroxyapatite (HA) crystals, similar to the dental enamel microstructure. ANOVA procedure showed significant effect of peptide treatment on the calculated SMR% ($p < 0.001$). Tukey's test revealed that peptide treated groups had significantly higher values of SMR%. In conclusion, LRAP is able to regulate the formation of HA and enhances the remineralization of acid-etched enamel as a surface treatment agent. SCANNING 37:179–185, 2015.

Key words: biomimetic, enamel, LRAP, remineralization, atomic force microscopy

Contract grant sponsor: Tehran University of Medical Sciences & Health Services; Contract grant number: 91-02-69-17777.

Conflicts of interest: The authors declare no potential conflicts of interest with respect to the publication of this study. This article is extracted from the results of the PhD thesis of the corresponded author.

*Address for reprints: Bagheri G. Hossein, Department of Dental Biomaterials, School of Dentistry/Research Center for Science and Technology in Medicine, Tehran University of Medical Sciences, Northern Kargar str., Hakim Highway, Tehran, Iran.
E-mail: hbagheri@hbagheri.com

Received 29 September 2014; Accepted with revision 2 December 2014

DOI: 10.1002/sca.21196
Published online 12 February 2015 in Wiley Online Library (wileyonlinelibrary.com).

Introduction

Dental Enamel is the most mineralized structure in the vertebrates, which is composed of at least 95% minerals. The microstructure of enamel is made up of well-organized carbonated hydroxyl apatite with some substitutions. The main portion of human enamel is nanorod-like calcium hydroxyapatite crystals, with the cross section of 25–100 nm and an undetermined length of about 100 nm to 100 μm or longer along the *c*-axis (Chen *et al.*, 2006). Since the constituting units of the

enamel crystal, consisting of ameloblasts and extracellular matrix, are removed after the enamel maturation, regeneration of damaged enamel is impossible. Therefore, biomimetic approaches were employed for synthesis of enamel-like structures (Du *et al.*, 2005, Palmer *et al.*, 2008, Chen *et al.*, 2013, Li *et al.*, 2014).

The hierarchical structure of enamel strongly affects its mechanical properties (Cui and Ge, 2007, Eimar *et al.*, 2012). It is suggested that the formation of enamel crystals undergoes two stages. At the first stage, the crystals elongate along their *c*-axes and parallel to each other. At the second stage, the crystals grow in width and become thicker into the nanofibrils (Boyde, '97). It is well known that the extracellular organic matrix plays an important role in the control of crystal growth, during the enamel mineralization (Robinson *et al.*, '89). The regulating effect of the organic matrix during the enamel formation is the consequence of the function of amelogenins, which form more than 90% of this organic matrix (Iijima and Moradian-Olda, 2004). Previous studies showed that the assembly of amelogenin, as nanospheres and chain-like structures (Aichmayer *et al.*, 2005), is essential for the regulatory role of amelogenin during enamel formation to affect the shape and arrangement of apatite crystals (Beniash *et al.*, 2005). However, some recent studies have brought up the probable importance of monomeric amelogenin peptides (Masica *et al.*, 2011; Tarasevich *et al.*, 2013).

There is an interest to produce remineralization systems for repairing enamel lesions via biomimetic approaches (Fan *et al.*, 2009; Tian *et al.*, 2012; Chen *et al.*, 2013; Li *et al.*, 2014). Among these attempts, the application of biologic peptides such as amelogenin is highly considered due to their biocompatibility (Kirkham *et al.*, 2007). Leucine-rich amelogenin peptide (LRAP) is the smallest of the amelogenin splice products, and is recognized as a signaling molecule which affects hard tissue mineralization (Boabaid *et al.*, 2004, Warotayanont *et al.*, 2009). Moreover, it has been shown to affect tooth germ development (Veis *et al.*, 2000). The presence of LRAP leads to changes in enamel appearance, compared to enamel from amelogenin null mice (Gibson *et al.*, 2009). Although some studies have shown that LRAP, which consists of N-terminal and C-terminal sequences of full-length amelogenin amino-acids (Fincham and Moradian-Oldak, '93; Habelitz *et al.*, 2006), cannot perform as structural peptides to regulate the apatite formation, but there are evidences for the regulation of the mineralization by LRAP (Le Norcy *et al.*, 2011).

The regulating role of LRAP on the hydroxyapatite mineralization is well described by Le Norcy *et al.* (2011). They have described the formation hydroxyapatite bundles in the presence of 2 mg/mL LRAP at physiologic conditions. The aim of this study was to investigate the assembly of these bundles by atomic force microscopy (AFM) and the influence of LRAP on the remineralization of artificial enamel defects. The null hypothesis was that the surface treatment of acid-etched enamel surface with LRAP would not affect the magnitude of surface microhardness recovery after immersing in remineralization solution.

Materials and Methods

Preparation of Peptide Solution

Porcine LRAP was synthesized commercially (GL Biochem Ltd., Shanghai, China) with the purity of 98% and free N- and C-terminal amino acids. The peptide was not phosphorylated on Ser-16, according to the previous findings (Le Norcy *et al.*, 2011). Peptide solution prepared as described by Le Norcy *et al.* (2011) in brief, 5 mg/mL stock solutions of lyophilized peptide were prepared using distilled de-ionized water (DDW) at room temperature (pH = 3.2). Peptide stock solutions were centrifuged (11000*g*, 4 °C, 20 min) prior to use.

Mineralization Experiments

Stock solutions of anhydrous calcium chloride (1M) (Merck, Germany) and sodium di-hydrogen phosphate (1M) (Merck, Germany) were prepared in deionized distilled water and filtered using 0.22-μm filters (JET BIOFIL, Guangzhou, China) prior to further use. Aliquots of peptide and calcium chloride solution were used to prepare solutions (pH = 7.2), with final concentrations of 1 or 2 mg/mL LRAP and 2.5 mM Ca^{+2}, using a micropipette. Aliquot of phosphate stock solution used to obtain final Ca/P molar ratio of 1.67. Potassium hydroxide (0.1 M) was used to adjust the final pH of each solution at pH = 7.2 immediately. The solutions were incubated at 37 °C for 24 h in sealed microtubes.

Transmission Electron Microscopy (TEM) and Selected Area Electron Diffraction (SAED)

TEM and SAED were used to confirm the formation of hydroxyapatite bundles as described before (Le Norcy *et al.*, 2011). After 24 h of incubation at 37 °C, 5 μL of the mineralization solution placed on Cu-grids after ultrasonic dispersion for 10 min. TEM analysis (Philips-CM30) was conducted at 250 kV for selected mineralization samples after 24 h.

To characterize the crystallization of the experiment products, Selected Area Electron Diffraction (SAED) was conducted using the above-described TEM device at 250 kV and diffraction patterns were captured by a CCD camera (AMT, Danvers, M.A., U.S.A.). Images

were analyzed using ImageJ 1.43 u software (NIH, Bethesda, M.D., U.S.A.).

Atomic Force Microscopy (AFM)

Five microliter of mineralization solution were placed on glass slides and dried at 37 °C. Atomic force micrographs were obtained using a NanoWizard II BioAFM (JPK Instrument AG, Berlin, Germany) in the intermittent-contact mode. Images were processed using JPK Data processing software version spm-3.4.15

Study the Surface Microhardness Recovery

Eighteen fresh bovine incisors were cut about 2 mm below the cementoenamel junction (CEJ) and embedded in poly methyl methacrylate resin, so that the buccal surface was exposed. The exposed surface of each specimen was polished using 600, 800, 1000, 1500, and 2000-grit sandpaper consequently to produce a polished flattened surface. The surface was painted with nail varnish, except for a working zone of $3 \times 3\ mm^2$.

Vickers microhardness (VMH) of the exposed area was measured (V-Test II Basic, Baresiss, Germany) before demineralization on the sound enamel (S-VMH), after demineralization (D-VMH) and after remineralization (R-VMH). Each measurement was included three indentations, using a 20 g load for 10 s. The working zone on each specimen was demineralized by acid etching, using 37% phosphoric acid solution for 30 s and washed thoroughly by deionized distilled water (DDW) (Cao *et al.*, 2014; Ruan and Moradian-Oldak, 2014). Before remineralization, one drop of 1 or 2 mg/mL ($n = 6$ for each concentration) of peptide solution was applied on the working surface and incubated for 30 min at 37 °C. Then, the specimens were immersed in remineralization solution, containing 2.5 mM Ca^{+2} and 1.5 mM PO_4^{-3} at 37 °C for 24 h. R-VMH numbers were measured after cleaning the working surface for 20 min in ultrasonic to remove any precipitations on the surface. Six samples were prepared and studied without application of peptide solution as control groups.

The surface microhardness recovery (SMR%) was calculated for each specimen as follows:

$$SMR\% = \frac{RVMH - DVMH}{SVMH - DVMH} \times 100$$

Field Emission Scanning Electron Microscopy (FE-SEM)

Bovine incisors were embedded in PMMA resin with the buccal surface exposed to the surface. Each surface was divided into three zones in the incisal–gingival direction. The first zone was painted using nail varnish as the sound enamel (SEn). The second zone was etched as described above and coated by nail varnish as the demineralized zone (DemEn) and the middle part was remained unpainted for remineralization. The prepared samples were immersed in remineralization solution with or without application of 2 mg/mL peptide primer ($n = 3$ for each). One sample of each experiment was selected randomly and prepared for FE-SEM study. A notch was created at the back of each block and the remained thickness was fractured using a chisel and cleaned in an ultrasonic bath for 15 min.The prepared cross sections of samples were gold sputtered and studied using Hitachi SE-4160 FE-SEM unit.

A one-way analysis of variance was used to study the effect of peptide concentration on the SMR%. Tukey's *post hoc* test was conducted for multiple comparisons consequently.

Results

TEM showed the formation of bundles (primary bundles) with the width of about 30 nm and the length of about 200 nm at 37 °C after 24 h in the presence of 1 and 2 mg/mL LRAP, which joined together to make secondary bundles (Fig. 1(A and B)). The white arrow

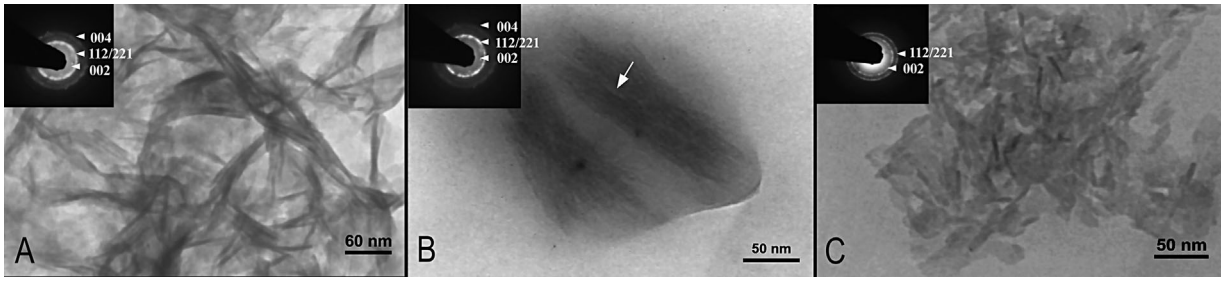

Fig 1. Transmission electron microscopy results of mineralization solution using 1 mg/mL (A), 2 mg/mL (B) LRAP solution and no peptide treatment (C). The crystals are organized in bundles, in the presence of LRAP. (A, B). SAED analysis shows crystalline pattern of HA in all solutions. Mineralization without LRAP shows no organization in HA crystals (C).

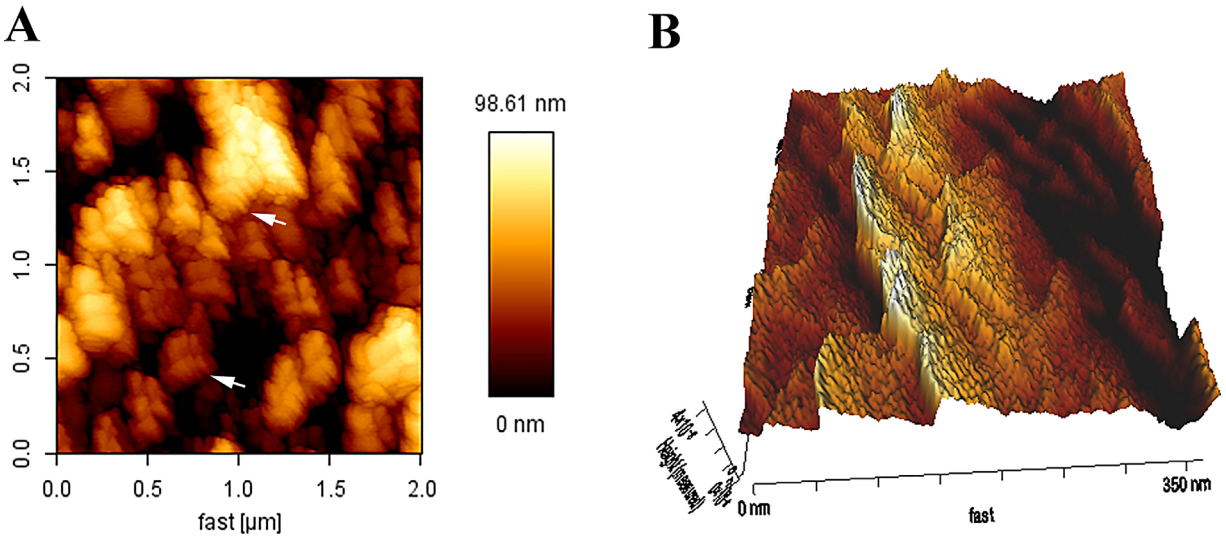

Fig 2. Height-measured mode of AFM imaging shows the hierarchical structure of dried material on the glass slide. (A) A coherent arrangement of secondary bundles composed of primary bundles (white arrows) is shown. Parallel secondary bundles with the length of about 400 nm are arranged longitudinally to form higher structures. 3D view of AFM imaging shows the hierarchical alignment of HA nano crystals in primary bundles (B).

in Figure 1(B) indicates primary bundles of about 30 nm wide, which join to form secondary structures. The primary bundles were composed of highly aligned nano fibers with the thickness of 2.21 ± 0.47nm ($n = 10$) (Fig. 2). SAED showed diffraction pattern, relating to the hydroxyapatite crystalline structure. Mineralization experiment in the absence of LRAP showed no organization and certain alignment of HA crystals (Fig. 1(C))

AFM revealed parallel arrays of about 50–80 nm thick and about 200 nm long which joined to compose higher structures with the diameter of about 400 nm after deposition on the glass surface (Fig. 2(A)). 3D processing of AFM images showed aligned structural units (primary and secondary bundles), which are composed of 2–4 nm crystal fibers (Fig. 2(B)). Similar to TEM, AFM showed that the crystal fibers were highly aligned in a parallel manner (Fig. 2(B)).

Effect of LRAP on the Surface Microhardness Recovery

The mean values for S-VMH, D-VMH, R-VMH, and SMR% are presented in Table I. Maximum SMR% was observed after using 2 mg/mL LRAP, while the specimens without peptide treatment showed the least SMR%. One-way ANOVA showed that peptide concentration had significant effect on SMR% ($p < 0.001$). Therefore, the null hypothesis must be rejected. Tukey's multi-comparison analysis showed that there was no significant difference in SMR% between 1 and 2 mg/mL LRAP. However, compared to the control group, the increase in the SMR% using 1 or 2 mg/mL LRAP was statistically significant ($p < 0.001$ for both).

When the specimens were not impregnated with the peptide solution, FE-SEM imaging showed an irregular precipitation of minerals on the surface (Fig. 3(C and E)). However, application of peptide solution on the etched enamel surface led to a regular crystal growth (Fig. 3(B and D)).

Discussion

In the present study, the ability of LRAP to form apatite assemblies and its effect on the remineralization of dental enamel were evaluated. There is an inconsistency in the literature about the LRAP assembly. Some studies have shown that LRAP exists as monomer in physiologic conditions (Tarasevich *et al.*, 2010, 2013), while there are some direct evidences for the formation of nano-spherical (Habelitz *et al.*, 2006; Le Norcy *et al.*, 2011) and chain-like LRAP assemblies(Le Norcy *et al.*, 2011). In the present study, the assembly of LRAP has not

TABLE I Mean (SD) values for sound, demineralized and remineralized enamel, as well as SMR% are reported for different groups

		Peptide concentration	
	Control	1 mg/mL	2 mg/mL
Sound VMH	321.62 (15.50)	332.58 (21.25)	332.54 (13.71)
DEM VMH	124.13 (11.25)	119.07 (15.65)	129.98 (6.27)
REM VMH	141.73 (8.08)	179.75 (17.69)	197.17 (10.78)
VMH Recovery	9.00 (4.26)	28.42 (7.16)	33.17 (11.97)

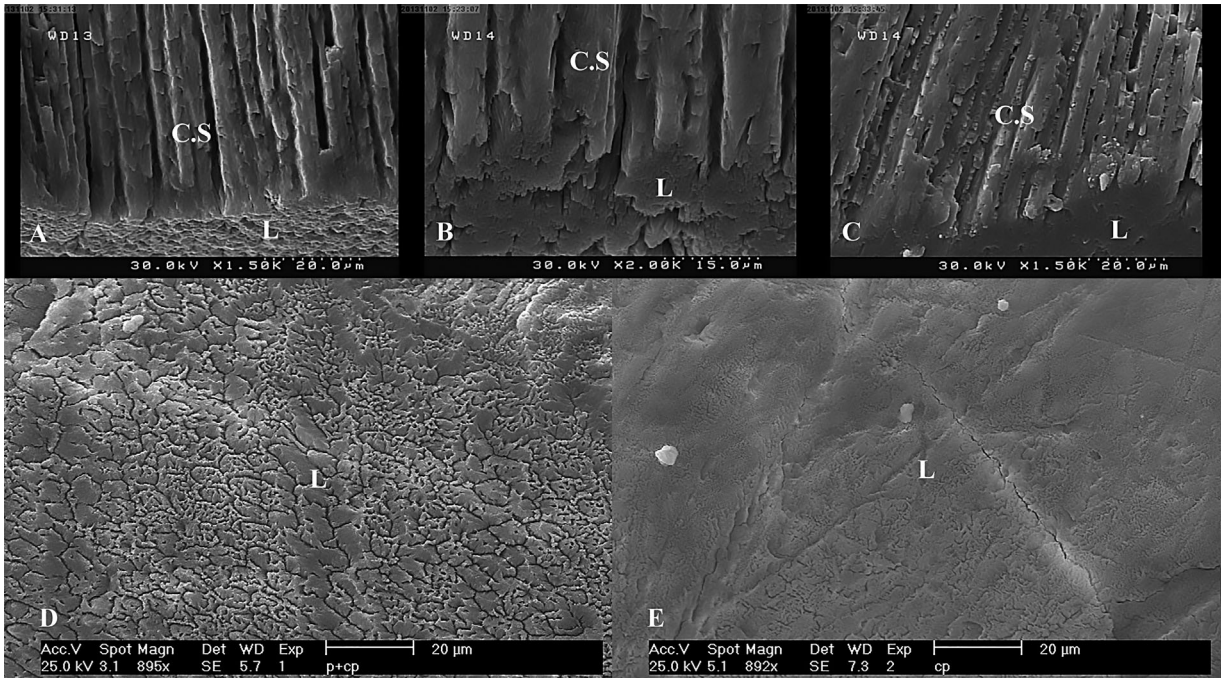

Fig 3. FE-SEM imaging of enamel samples after demineralization (A) and remineralization using 2 mg/mL LRAP surface primer (B and D) and without peptide treatment (C and E). Application of LRAP caused well-guided crystal growth (B). Without peptide treatment, the crystal growth occurred, lacking any pattern. (C) (L, Labial surface; C.S., Cross sectional plan).

been studied; however, it has notably altered the pattern of crystal growth in super-saturated calcium phosphate solution. Both theories about the form of LRAP assembly can justify the regulation of HA formation as it was observed in the present TEM and SAED experiments (Fig. 1). If LRAP assembles as nanospheres and forms chain-like structures, these chains can perform like a scaffold for crystal growth (Le *et al.*, 2006, Fan *et al.*, 2011). Moreover, calcium ions may influence the peptide assembly, since it was reported that Ca^{+2} ions may lead to the aggregation of acidic proteins to form a crystal growth template in dentin (He *et al.*, 2003). On the other hand, if the dominant form of LRAP is considered as monomers, the formation of elongated crystals can be relevant to the selective adhesion of LRAP on the certain HA faces, in a such manner that it allows the crystal growth in the c-axis direction(Habelitz *et al.*, 2006; Le Norcy *et al.*, 2011; Masica *et al.*, 2011). The electron diffraction pattern in this study, having distinguished diffraction pattern relating to the (002) and (004) plans, indicated that the HA fibers are aligned along their c-axis (He*et al.*, 2003; Le Norcy *et al.*, 2011).

AFM showed repeating structures, having the dimensions of bundles in TEM images, which can propose that these structures may be the HA bundles. Regarding the human enamel hierarchical structure, the primary bundles in the present study are comparable with the enamel nanofibrils in their width (about 30 nm), or enamel nanorods as described previously (Kerebel *et al.*, 1979; Cui and Ge, 2007). The nanofibrils (or nanorods) are the basic structural units of the human enamel. In agreement with previous studies (Kerebel *et al.*, 1979; Cui and Ge, 2007), the major components of nanofibrils (or primary bundles in this study) are hydroxyapatite crystals, while their *c*-axes are preferentially oriented along the long axis of the nanofibrils. Furthermore, the aggregation behavior of the primary bundles to form "secondary bundles" are similar to these nanofibrils which bind together to form fibrils of about 80–130 nm thick (Cui and Ge, 2007). In the present study, while the solution is being dried, Brownian motion will help the bundles to join together preferentially in a parallel orientation, to achieve a low-energy configuration (Banfield *et al.*, 2000). In earlier studies (Jiang and Liu, 2004; Wang *et al.*, 2008), it has been suggested that amelogenin-calcium phosphate nanoparticles aggregate via oriented attachment to make parallel orientations and consequently form nanorods (primary bundles in this study). Finally, these nanorods self-assemble into higher microstructures as described in the present study. However, as the fibrils and nanofibrils are nearly perpendicular to the surface, they appear as particle in AFM images (Cui and Ge, 2007).

Some previous studies have shown that the treatment of demineralized enamel by Asp-Ser-Ser (Chung and Huang, 2013; Chung and Li, 2013a,b; Yang *et al.*, 2014) or amelogenin (Fan *et al.*, 2011) promotes enamel remineralization. Moreover, the ability of casein phosphopeptides to improve enamel remineralization

is well proven (Reynolds, '97; Mehta *et al.*, 2014; Zhou *et al.*, 2014). Proteins can bind to crystal faces to accelerate or inhibit crystal growth(Shiraga *et al.*, '92). In the present study, the recovery of surface microhardness was increased after peptide treatment. In the literature, there are decisive evidences for the adsorption of LRAP onto the HA crystal surface (Tarasevich *et al.*, 2010; Masica *et al.*, 2011). It has been shown that LRAP adsorbs from physiologic solution as monomer (Tarasevich *et al.*, 2010, 2013). The ability of a peptide segment to bind to the HA surfaces depends on the number and position of the charges. Those segments, with several negative charges, show high affinity for binding to calcium, probably by chelating the calcium ions on the surface, whereas positive or neutral parts bind less strongly to HA (Meyer and Nancollas, '73). Therefore, it would not be so surprising, if LRAP binds to HA surface, since it has plenitude of acidic amino acids (i.e., aspartic acid and glutamic acid) in its sequence. Similarly, Kirkham *et al.* (2007) reported the increased calcium and phosphate uptake of peptide-treated enamel samples. Furthermore, thermodynamic study showed that the LRAP has about 6.4 times more affinity for bonding to Ca^{+2} ions in comparison with the amelogenin (Le *et al.*, 2006). Therefore, the LRAP can also act as a reservoir for calcium ions more effectively than amelogenin and may be more effective to be used for a biomimetic remineralization system.

According to what discussed above, by peptide treatment, LRAP binds to specific faces of hydroxyapatite crystals (Tarasevich *et al.*, 2013) and covers the enamel prisms. Acid-etching using phosphoric acid is a simple and convenience method to create erosion-like lesions in enamel (Ruan and Moradian-Oldak, 2014). It dissolves the superficial enamel as-well as underlying enamel prisms selectively, creating a superficial lesion with the depth of about 20 μm (Månson-Rahemtulla *et al.*, '84), which reduces the enamel hardness. After soaking in the remineralization solution, as the exposed crystals are coated by peptide, adsorption of calcium ions onto the enamel crystals will be promoted and the crystal growth will occur in the c-axis direction. This can lead to enhanced, as well as, guided regrowth and reconstruction of enamel prismatic structure, as represented in this study by SEM and SMR%. SEM showed the effect of LRAP on the pattern of remineralization (Fig. 3). Treatment of etched enamel surface by LRAP led to an orchestrated regrowth of enamel crystals.

Conclusion

This study shows that LRAP surface treatment can be used to promote biomimetic remineralization of enamel for probable preventive and non-invasive therapeutic applications. Since the production of LRAP is less complicated, with lower expense in comparison with the full-length amelogenin, these results may be promising for the clinical use in the future.

References

Aichmayer B, Margolis HC, Sigel R, et al. 2005. The onset of amelogenin nanosphere aggregation studied by small-angle X-ray scattering and dynamic light scattering. J Struct Biol 151:239–249.

Banfield JF, Welch SA, Zhang H, Ebert TT, Penn RL. 2000. Aggregation-based crystal growth and microstructure development in natural iron oxyhydroxide biomineralization products. Science 289:751–754.

Beniash E, Simmer JP, Margolis HC. 2005. The effect of recombinant mouse amelogenins on the formation and organization of hydroxyapatite crystals in vitro. J Struct Biol 149:182–190.

Boabaid F, Gibson CW, Kuehl MA, et al. 2004. Le ucine-rich amelogenin peptide: a candidate signaling molecule during cementogenesis. J Periodontol 75:1126–1136.

Boyde A. 1997. Mic rostructure of enamel. Ciba Found Symp 205:18–27; discussion 27–31.

Cao Y, Mei ML, Li Q-L, Lo ECM, Chu CH. 2014. Enamel prism-like tissue regeneration using enamel matrix derivative. J Dent In press (0).

Chen H, Tang Z, Liu J, et al. 2006. Ac ellular Synthesis of a Human enamel-like microstructure. Adv Mater 18:1846–1851.

Chen L, Liang K, Li J, et al. 2013. Regeneration of biomimetic hydroxyapatite on etched human enamel by anionic PAMAM template in vitro. Arch Oral Biol 58:975–980.

Chung H-Y, Huang K-C. 2013. Effects of peptide concentration on remineralization of eroded enamel. J Mech Behav Biomed Mater 28:213–221.

Chung H-Y, Li C-C. 2013a. As paragine–serine–serine peptide regulates enamel remineralization in vitro. J Mater Res 28:2890–2896.

Chung H-Y, Li C-C. 2013b. Microstructure and nanomechanical properties of enamel remineralized with asparagine–serine–serine peptide. Mater Sci Eng C 33:969–973.

Cui FZ, Ge J. 2007. New observations of the hierarchical structure of human enamel, from nanoscale to microscale. J Tissue Eng Regen Med 1:185–191.

Du C, Schneider GB, Zaharias R, et al. 2005. Apatite/amelogenin coating on titanium promotes osteogenic gene expression. J Dent Res 84:1070–1074.

Eimar H, Ghadimi E, Marelli B, et al. 2012. Regulation of enamel hardness by its crystallographic dimensions. Acta Biomater 8:3400–3410.

Fan Y, Nelson JR, Alvarez JR, et al. 2011. Amelogenin-assisted ex vivo remineralization of human enamel: effects of supersaturation degree and fluoride concentration. Acta Biomater 7:2293–2302.

Fan Y, Sun Z, Moradian-Oldak J. 2009. Controlled remineralization of enamel in the presence of amelogenin and fluoride. Biomaterials 30:478–483.

Fincham AG, Moradian-Oldak J. 1993. Amelogenin post-translational modifications: carboxy-terminal processing and the phosphorylation of bovine and porcine "TRAP" and "LRAP" amelogenins. Biochem Biophys Res Commun 197:248–255.

Gibson CW, Li Y, Daly B, et al. 2009. The leucine-rich amelogenin peptide alters the amelogenin null enamel phenotype. Cells Tissues Organs 189:169–174.

Habelitz S, DenBesten PK, Marshall SJ, Marshall GW, Li W. 2006. Self-assembly and effect on crystal growth of the leucine-rich amelogenin peptide. Eur J Oral Sci 114(s1):315–319.

He G, Dahl T, Veis A, George A. 2003. Nucleation of apatite crystals in vitro by self-assembled dentin matrix protein 1. Nat Mater 2:552–558.

Iijima M, Moradian-Oldak J. 2004. Interactions of amelogenins with octacalcium phosphate crystal faces are dose dependent. Calcif Tissue Int 74:522–531.

Jiang H, Liu XY. 2004. Principles of mimicking and engineering the self-organized structure of hard tissues. J Biol Chem 279:41286–41293.

Kerebel B, Daculsi G, Kerebel LM. 1979. Ul trastructural studies of enamel crystallites. J Dent Res 58(Spec Issue B):844–851.

Kirkham J, Firth A, Vernals D, et al. 2007. Self-assembling peptide scaffolds promote enamel remineralization. J Dent Res 86:426–430.

Le Norcy E, Kwak SY, Wiedemann-Bidlack FB, et al. 2011. Leucine-rich amelogenin peptides regulate mineralization in vitro. J Dent Res 90:1091–1097.

Le TQ, Gochin M, Featherstone JD, Li W, DenBesten PK. 2006. Comparative calcium binding of leucine-rich amelogenin peptide and full-length amelogenin. Eur J Oral Sci 114-(s1):320–326.

Li Q-L, Ning T-Y, Cao Y, et al. 2014. A novel self-assembled oligopeptide amphiphile for biomimetic mineralization of enamel. BMC Biotechnol 14:32.

Månson-Rahemtulla B, Retief DH, Jamison HC. 1984. Effect of concentrations of phosphoric acid on enamel dissolution. J Prosthet Dent 51:495–498.

Masica DL, Gray JJ, Shaw JWJ. 2011. Partial high-resolution structure of phosphorylated and non-phosphorylated leucine-rich amelogenin protein adsorbed to hydroxyapatite. J Phys Chem C 115:13775–13785.

Mehta AB, Veena Kumari RJ, Izadikhah V. 2014. Remineralization potential of bioactive glass and casein phosphopeptide-amorphous calcium phosphate on initial carious lesion: An in-vitro pH-cycling study. J Conserv Dent 17:3.

Meyer JL, Nancollas GH. 1973. The influence of multidentate organic phosphonates on the crystal growth of hydroxyapatite. Calcif Tissue Res 13:295–303.

Palmer LC, Newcomb CJ, Kaltz SR, Spoerke ED, Stupp SI. 2008. Biomimetic systems for hydroxyapatite mineralization inspired by bone and enamel. Chem Rev 108:4754–4783.

Reynolds E. 1997. Remineralization of enamel subsurface lesions by casein phosphopeptide-stabilized calcium phosphate solutions. J Dent Res 76:1587–1595.

Robinson C, Kirkham J, Stonehouse NJ, Shore RC. 1989. Control of crystal growth during enamel maturation. Connect Tissue Res 22:139–145.

Ruan Q, Moradian-Oldak J. 2014. Development of amelogenin-chitosan hydrogel for in vitro enamel regrowth with a dense interface. J Vis Exp 89:e51606.

Shiraga H, Min W, VanDusen W, et al. 1992. Inhibition of calcium oxalate crystal growth in vitro by uropontin: another member of the aspartic acid-rich protein superfamily. Proc Natl Acad Sci 89:426–430.

Tarasevich BJ, Lea S, Shaw WJ. 2010. The leucine rich amelogenin protein (LRAP) adsorbs as monomers or dimers onto surfaces. J Struct Biol 169:266–276.

Tarasevich BJ, Perez-Salas U, Masica DL, et al. 2013. Neutron reflectometry studies of the adsorbed structure of the amelogenin, LRAP. J Phys Chem B 117:3098–3109.

Tian K, Peng M, Ren X, Liao C, Fei W. 2012. Regeneration of tooth-like hydroxyapatite depended on amelogenin functional section monolayer: a new approach for tooth repair. Med Hypotheses 79:143–146.

Veis A, Tompkins K, Alvares K, et al. 2000. Specific amelogenin gene splice products have signaling effects on cells in culture and in implants in vivo. J Biol Chem 275:41263–41272.

Wang L, Guan X, Yin H, Moradian-Oldak J, Nancollas GH. 2008. Mimicking the self-organized microstructure of tooth enamel. J Phys Chem C Nanomater Interfaces 112:5892–5899.

Warotayanont R, Frenkel B, Snead ML, Zhou Y. 2009. Leucine-rich amelogenin peptide induces osteogenesis by activation of the Wnt pathway. Biochem Biophys Res Commun 387: 558–563.

Yang Y, Lv X, Shi W, et al. 2014. 8Dss-promoted remineralization of initial enamel caries in vitro. J Dent Res 93:520–524.

Zhou C, Zhang D, Bai Y, Li S. 2014. Casein phosphopeptide–amorphous calcium phosphate remineralization of primary teeth early enamel lesions. J Dent 42:21–29.